AQUA
Water Infrastructure, Ecosystems and Society

IWA PUBLISHING

 AQUA — Water Infrastructure, Ecosystems and Society Vol 71 No 5, 593 doi: 10.2166/aqua.2022.136

Multi-objective operational optimization toward improved resilience in water distribution systems

Chao Zhang[a], Haixing Liu[a,*], Shengwei Pei[b], Mengke Zhao[a] and Huicheng Zhou[a]

[a] School of Hydraulic Engineering, Dalian University of Technology, Dalian 116023, China
[b] Centre for Water Systems, University of Exeter, Exeter EX4 4QF, UK
*Corresponding author. E-mail: hliu@dlut.edu.cn

ABSTRACT

Resilience has currently attracted increasing interest in the optimization of water distribution systems (WDSs). Most research mainly focuses on optimal design problems. However, the system operation has not been investigated adequately regarding resilience. Therefore, we proposed an integral format of the demand-weighted modified resilience index (IMRI), which can capture the overall resilient performance throughout the operational period. This indicator was incorporated into the multi-objective operation optimization model as one of the objectives. Two benchmark networks were considered as case studies. The resulting Pareto fronts show a clear competing relationship between cost and resilience. Operating conditions in pumps, reservoirs and tanks at each regulation step were characterized by methods of resilience decomposition, which proved valuable intuitively for resilience regulation. A framework for explicit resilience assessment was also developed to examine directly the overall performance in statistics about those optimal solutions obtained. Explicit resilience results show that the IMRI can effectively quantify the resilience of system operation in the temporal dimension. Furthermore, scheduling more pumps, higher trigger-on levels of tanks and a wider range of trigger-level control could yield a more resilient solution to the operation of WDSs.

Key words: multi-objective optimization, operation, pipe failure, resilience, water distribution systems

HIGHLIGHTS

- A multi-objective optimization with resilience was proposed to guide the resilient operation in WDSs.
- A method of resilience decomposition was developed for comparison of operating conditions in WDSs.
- A framework of explicit resilience analysis under pipe failures was built, where three metrics are designed to quantify the operational performance directly.

GRAPHICAL ABSTRACT

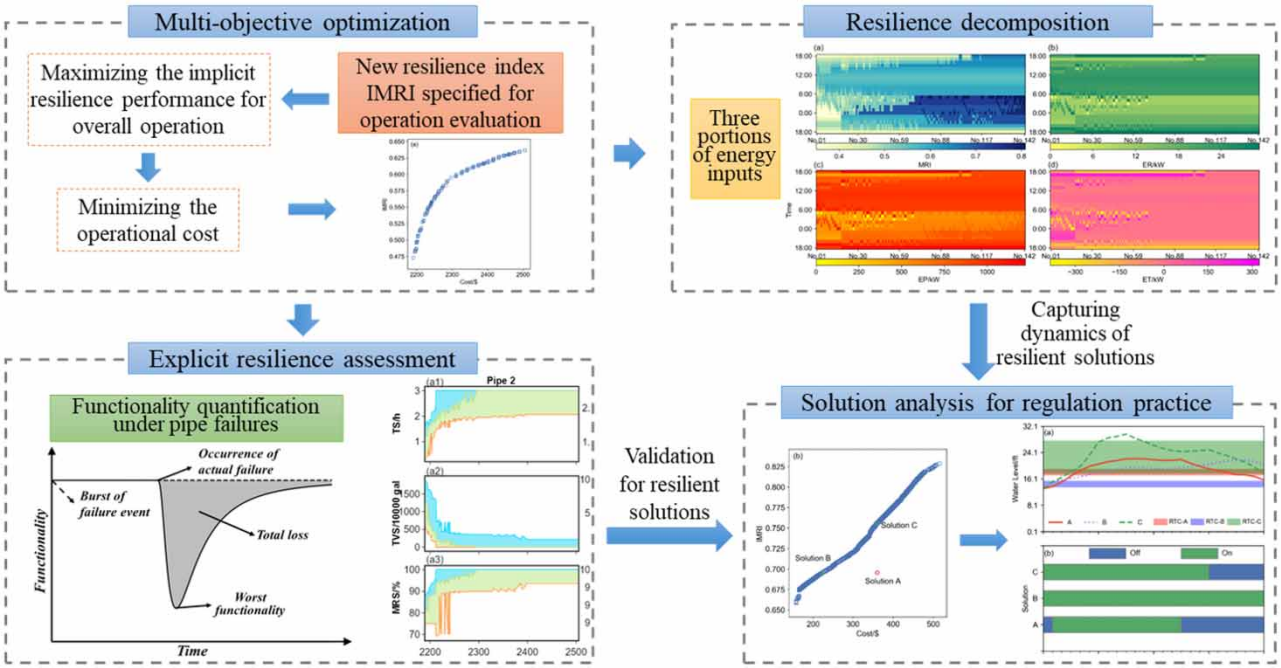

INTRODUCTION

Water distribution system (WDS) operation issues have gained much attention since it consumes considerable energy and led to a huge amount of operational costs. According to the USEPA, the energy consumption by drinking water and wastewater utilities accounts for 30–60% of total energy in the city (USEPA 2008). The operation optimization studies initially focus on the constrained single-objective optimization problems for minimizing the pumping cost. Although the efficiency of solving optimization problem has significantly improved by various advanced algorithms (Coulbeck *et al.* 1987; Zessler & Shamir 1989; Brion & Mays 1991; Brdys & Chen 1995; Wegley *et al.* 2000; López-Ibáñez *et al.* 2008), the optimized solution sorely pursuing the least cost tends to provide less choices (e.g., reliability, resilience, risk) for decision-makers to implement. In practice, a trade-off in many alternative solutions is much more preferred, in which the operational cost and system performance could be better balanced (Haimes 2015).

Since WDSs have been challenged by various threats throughout the world, including climate change, population growth and rapid urbanization, the provision of more reliable, resilient and sustainable water management is required (Butler *et al.* 2017). Thus, it becomes essential that system performance should be incorporated into the operation analysis in WDSs, especially the multi-objective optimization. There are considerable methods for system performance assessment, for example, robustness (Kapelan *et al.* 2005), risk (Lopes *et al.* 2012), resilience (Todini 2000) and reliability (Damelin *et al.* 1972).

Resilience is a widely investigated infrastructure performance assessment in recent years. The resilience concept, originally from the ecological field (Holling 1973), refers to the capability of the system to overcome failure condition. Based on this conception, there emerge a great number of quantitative indicators with simple expressions. Todini (2000) first proposed the quantitative indicator – the Resilience Index (RI), which is defined as the ratio of surplus nodal energy to the energy dissipated internally in the system. Later, Prasad & Park (2004) introduced the node uniformity coefficient into the RI to integrate the effect of the looped network, termed as the network resilience index (NRI). The minimum surplus head is considered as a surrogate indicator for resilience evaluation (Farmani *et al.* 2005). The modified Resilience Index (MRI) (Jayaram & Srinivasan 2008), mixed reliability surrogate (Raad *et al.* 2010), flow entropy (Atkinson *et al.* 2014), Diameter-Sensitive Flow Entropy (DSFE) (Liu *et al.* 2014), the Available Power Index (API) and the Pipe Hydraulic Resilience Index (PHRI) (Liu *et al.* 2016) also enriched the context of resilience metrics in WDSs.

These measures are successfully applied to the evaluation for water network design, but few researches pay attention to their application to performance assessment for system operation. Zhuang *et al.* (2012) conducted a resilience analysis for pump and valve operation under the pipe failure conditions, with system availability as the measure of resilience. Diao *et al.* (2016) presented a global resilience analysis framework to implement the assessment over extended periods and measured both strain magnitude and duration under a great many failure scenarios. Odan *et al.* (2015) developed a real-time operational optimization framework in WDSs, where the MRI was used as the optimal objective to evaluate system resilience. These several studies mainly concern the effects of operational interventions on system resilience, but the relationship between operational cost and system resilience is not fully investigated further, which should not be ignored to support decision-makings in practice.

Motivated by these investigations aforementioned, this paper lays emphasis on trade-offs between cost and resilience in WDSs' operation. Aiming for that, an integral format of demand-weighted MRI (IMRI) is proposed as the objective to evaluate the overall resilient performance over an extended period simulation (EPS). Resilience decomposition is developed to give insight into this relationship. Besides, the posterior evaluation under the framework of explicit resilience assessment is conducted to verify the resilience performance of optimal solutions.

The rest of this paper is structured as follows. First, the multi-objective optimization model for operation in WDSs is presented, of which the objectives are the minimization of the operational cost and the maximization of the IMRI. Then, the Pareto-optimal solutions are obtained by solving this problem through the well-known NSGA-II algorithm. Afterward, the comparison of optimal solutions is implemented according to resilience decomposition and explicit assessment. Finally, applications to two benchmark cases are demonstrated and conclusions are drawn.

METHODOLOGY

Resilience assessment

Although there are many evaluable indicators applied to resilience assessment in WDSs, they cannot be directly used in the issue of system operation over EPS. Hence, a new resilience indicator specially formulated for operation assessment, is introduced elaborately below.

The MRI presented here is selected as the base indicator of the IMRI, which was initially proposed by Jayaram & Srinivasan (2008), which can be utilized effectively in resilience assessment for the WDS of multi-sources. From Equation (1) it is expressed as the ratio of the surplus energy for demand nodes to the required energy.

$$\mathrm{MRI} = \frac{\sum_{j}^{nn} \gamma Q_j^{req}(H_j - H_j^{req})}{\sum_{j}^{nn} \gamma Q_j^{req} H_j^{req}} \tag{1}$$

where H_j, H_j^{req} and Q_j^{req} are the actual head, the minimum head for requirement and the required flow rate at the jth demand node, respectively; γ is the specific weight of water; nn is the number of demand nodes.

In comparison to the MRI, other resilience indicators such as the RI, the NRI and the API follow a similar formula. They take a format of ratio, but all include energy portions from pumps and reservoirs in the formula denominator. This may induce inconsistent assessment in the WDS controlled by pump stations. In such a system, the more energy pumping into pipelines, the more surplus energy available for water supply. It is expected to attain a better performance in resilience assessment, but the calculated values in these indicators may attain a lower level, merely because of the high value of energy portion from pumps in the denominator. Conversely, the surplus head is the sole factor determining the quantification of the MRI, once the head requirements are definite. The surplus head is positively correlated to resilience (Farmani *et al.* 2005). In this regard, the MRI can be theoretically effective in resilience assessment regardless of variations of hydraulics. This special feature is exactly suited to the resilience assessment in operation with dynamic hydraulic conditions.

To evaluate the overall performance of operational solutions during EPS, the IMRI is defined as an integral of nodal demand-weighted MRI here. Due to the time-variant operating conditions, a unique MRI value at a certain time-point cannot reflect availably the resilience assessment of operational controls. Meanwhile, in the control decision-makings of the WDS, the resilience performance during peak-demand period plays a key role. Therefore, as shown in Equation (2),

the mathematical expression of the IMRI is given as

$$\mathrm{IMRI} = \frac{\int_0^T \mathrm{MRI} \times Q dt}{\int_0^T Q dt} \tag{2}$$

where T is the time duration of EPS; Q is the total required demand of system. The value can be calculated by the rate of sum of nodal demand-weighted MRI values by a hydraulic step to the total demand over EPS. The higher value of IMRI the regulation control for the WDS gets, the more energy the WDS overall provides to demand nodes, which can be seen as the better behavior in terms of resilience.

Model formulation

Objective functions

The first objective used in this optimization model is the minimization of pumping cost in an operational cycle. Generally, the operational cost is comprised of energy consumed and maintenance expense. Because it is difficult to quantify the maintenance cost and the energy consumed accounts for up to 90% of operational expense, only the pumping cost due to energy consumption is regarded as the objective in this paper. The cost objective is given as follows.

$$\text{Minimize } C_e = \frac{\sum_{i=1}^{ni} \sum_{j=1}^{np} \gamma u c_i Q_{ij} H_{ij} \Delta t_i}{\eta_{ij}} \tag{3}$$

where C_e is the total pumping cost during EPS; uc_i is the unit electricity tariff during the ith time interval; Q_{ij} and H_{ij} are the flow and head of pump j during the ith time interval, respectively; η_{ij} is the wire-to-water efficiency of pump j during the ith time interval; ni and np are the number of time intervals and operating pumps during EPS, respectively. Δt_i is the ith hydraulic step. The second objective here is the maximization of the IMRI, used to evaluate system performance in operation, which has been introduced above in Equation (2).

Constraints

Three constraints are set up in the pump operation optimization: (1) minimum nodal pressure requirement, (2) continuous operation of tanks and (3) switch times of pumps. The continuity equation at nodes and energy conservation are implicitly handled by the EPANET hydraulic simulator (Rossman 2000).

The goal of water utilities is to supply sufficient water with adequate pressure to users. Hence, the nodal pressure should be greater than the minimal pressure requirement at each demand node all the time, and the expression is given as,

$$H_{ij} \geq H_{ij}^{req} \quad i = 1, \ldots, n \; j = 1, \ldots, nn \tag{4}$$

where H_{ij} and H_{ij}^{req} are the actual head and the required head at the ith time point in the jth demand node; n is the number of time steps of EPS.

A 24-h period of EPS is used here. In order to guarantee the system operation continuum, tank level at the end of simulation should be higher than or equal to the initial level. The formula is given as:

$$WL_{sj} \leq WL_{ej} \quad j = 1, \ldots, nt \tag{5}$$

where WL_{sj} is the initial level in jth tank; WL_{ej} is the water level in jth tank at the end of EPS. nt is the number of tanks in a WDS.

Frequent switching of a pump will lead to wear-out failure and thus increasing the maintenance cost (Lansey & Awumah 1994). The number of pump switches should be lower than the maximum times allowed.

$$NS_j \leq NS_{max} \quad j = 1, \ldots, np \tag{6}$$

where NS_j and NS_{max} are the number of switches and the corresponding limitation for pump j.

Decision variables

In this study, two types of pump control rules are taken into account. The first one is the time-schedule for pump switches during EPS. So, the decision variables can be the number of operating pumps with the same type at each time interval. The other is the regulation rules for trigger-level settings which control pumps switched on/off through the monitor of real-time water levels. The pairs of trigger-on and trigger-off levels for a pump are the decision variables.

Optimization algorithm

The non-dominated sorting genetic algorithm II (NSGA-II) (Deb *et al.* 2002) has inspired a significant number of adoptions to the multi-objective optimization problems for WDS operation. (Barán *et al.* 2005; Kurek & Brdys 2006; Mala-Jetmarova *et al.* 2014). Since its applications have shown good performance in this field, this study uses NSGA-II to solve the optimization model. The NSGA-II develops a fast non-dominated sorting approach to reduce the computation burden radically. It uses a preservation strategy for elites to accelerate the convergence to Pareto-optimal set and designs a crowding distance method of maintaining the diversity in a population for each generation. Due to space limit, a full description of NSGA-II can be found in Deb *et al.* (2002) and will not be discussed emphatically in this paper.

Resilience decomposition

In this section, three energy metrics are set up based on decomposition for the formulation MRI, for the illustrations of features of operational solutions over EPS. They are quantified for elucidating the operating conditions in pumps, tanks and reservoirs. According to the energy conservation law, the power portions from reservoirs, pumps, and tanks are important indicators for resilience, since they constitute the entirety of the energy supplied to demand nodes for each time step in a WDS simulation. We denoted them as *ER*, *EP*, *ET*, respectively, in Equations (7)–(9).

$$ER = \sum_{j}^{nr} \gamma Q_j^r H_j^r \tag{7}$$

$$EP = \sum_{j}^{np} \gamma Q_j^p H_j^p \tag{8}$$

$$ET = \sum_{j}^{nt} \gamma Q_j^t H_j^t \tag{9}$$

where H_j^r and Q_j^r are the head and outflow in the reservoir j. H_j^p and Q_j^p are the head and outflow in the pump j. H_j^t and Q_j^t are the head and outflow in the tank j.

These three quantitative assessments can fundamentally characterize the variations of total input energy (Liu *et al.* 2016). It should be emphasized that the respective investigation of the dynamic conditions in reservoirs and tanks is critical. Energy from high-elevation reservoirs is the non-negligible dual source of energies in a gravity supply system. A tank can be thought of as either a feeding or a demanding node. While pumps shut down, tanks can supply energy to demand users. Note that when calculating *ET*, the direction of flow into tanks must be considered. That is, when tanks feed demand nodes, the quantity value of *ET* would be negative. Thus, unlike *ER* and *EP*, a lower *ET* value indicates a greater energy intake from tanks.

Explicit resilience assessment

The explicit resilience assessment framework for the WDS under failure scenarios, is presented here. Since the IMRI is a surrogate measure, system functionality responding to failures can be directly evaluated to verify the applicability of the IMRI. The provision of sufficient water under failure scenarios can explain the ability of a resilient system. In this regard, the assessment framework contains two main parts, which are listed in detail as follows.

- Simulation of the failure scenarios: In this assessment framework, pipe failures are taken as the modeling failure scenarios, which is part of main failure modes (Diao *et al.* 2016). Pipe burst events at water mains are selected as the base scenario due to its significance to water supply. Concerning the randomness of occurrence time over the operating period, the failure can start at all time points (generated by fixed time step) during EPS. Meanwhile, for simplification, the duration of failure is 3 h

and the detection for failure is neglected (Diao *et al.* 2016). The isolation for repairing pipe is only simulated in the scenario, so that the failed pipe is modeled by setting the status of pipe to closed for 3 h from the specified starting time.

- Evaluation of the performance in water provision: A time-varying curve of system functionality, as shown in Figure 1, depicts three typical development stages for a WDS in a failure event. In the stage of resistance, while a failure event occurs, there is a window time before the actual failure of system arises, when system functionality starts to be lower than the normal level. This time can reflect the ability of system sustaining the normal level of service. In the stage of deterioration, the functionality gradually decreases until it reaches the lowest point, which is the worst level of service to water users. It is always the most concern for water utilities. In the stage of recovery, the functionality starts to increase until it recovers to the initial level. The total loss marked by the shaded area over the time of the actual failure, can signify the overall deficit in system functionality. In the light of evaluation in supplying an adequate demand, system functionality can be regarded as the satisfactory level of water supply. When the pressure head for any water user is lower than the requirement, indicating the demand is not met, the water supply service is deemed to be below the normal level. Pressure-dependent demand (PDD) is utilized in the hydraulic solver (Morley & Tricarico 2008). Moreover, three assessment metrics for explicit resilience corresponding to the development stages aforementioned, are proposed below:

  - Time to Sustain (*TS*): Time between the starting time of a failure event and first occurrence time of deficient head at any demand node. Its value can be not higher than the duration of a pipe failure event. The greater values of *TS* suggest that the system can sustain normal water supply for a longer time, which represents better resilience performance.
  - Total Volume of water Shortage (*TVS*): The whole insufficient water volume at all demand nodes over the failure period. Its value could be less than the total required demand of all affected water users. The smaller value of TVS, reflecting less severe water shortage of the WDS till a full recovery, can manifest better resilience performance.
  - Minimum Ratio of water Supply (*MRS*): The minimum ratio of actual demand at all demand nodes to the required demand during the failure period. The value of this metric can reach at most 1.0. The higher value of *MRS* shows better resilience performance, which is often associated with a more satisfactory level of water supply service of system at the most deficit time point.

Case studies

Two networks, namely Anytown (Walski *et al.* 1987) and Net3 (Rossman 1993), are applied as study cases to verify the proposed methods.

Anytown – a typical looped system – was first used in the optimal design problem in the WDS (Walski *et al.* 1987). The original network is expanded by the best design solution in terms of cost solved by Farmani *et al.* (2005). As shown in Figure 2(a), the network contains three tanks, 63 pipes and 22 nodes, of which 19 demand nodes have the same peak-demand period (6:00–15:00) and off-peak-demand period (21:00–6:00). Only one pumping station lifts water from the low-head Reservoir 40 to users, with three identical pumps in parallel, where there are no regulation rules yet. The pressure head at all demand nodes is required over 40 psi. The aim of this case is to seek the optimal time-table schedule of three paralleled pumps during 24 h EPS.

Net3 case was initially developed by Rossman (1993). The network consists of 92 nodes, 117 pipes and three tanks, as shown in Figure 2(b). Two pump stations from different sources deliver water to users. Pump Station 335 has greater pumping

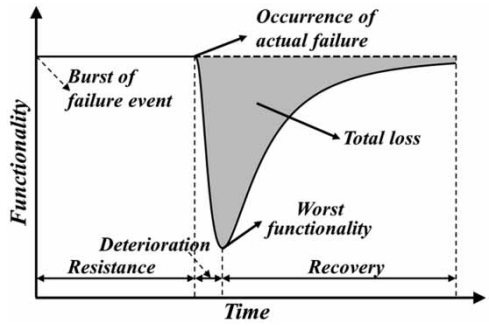

Figure 1 | Schematic drawing of time variation of system functionality in the failure event.

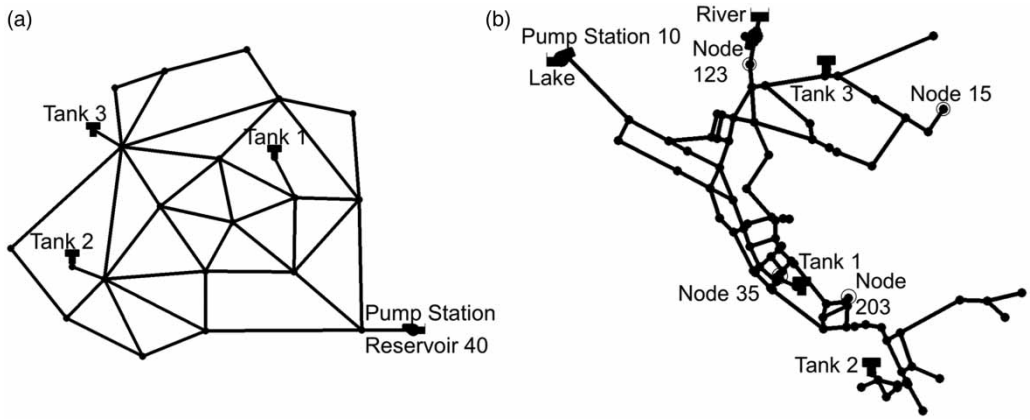

Figure 2 | Layouts of case networks: (a) Anytown and (b) Net3.

capacity and much higher head than Pump Station 10. Pump Station 10 has an existing time-schedule for operation. The regulation of Pump Station 335 is determined by water levels in Tank 1 through the trigger-on/off rules, whereas the status (open/closed) of bypass Pipe 330 is controlled by the same trigger levels in the inverse rules. There exists a base demand pattern for most demand nodes, of which the peak period is 22:00–04:00 and off-peak period is 04:00–07:00 and 18:00–22:00. The network should give guarantee of water supply at the minimum pressure head of 35 psi, especially at the Node 203 in system, of which the demand accounts for half of total demand of system. The aim of this case is to seek the optimal time-table schedule of Pump 10 during 24 h EPS and the pair of trigger levels for Pump Station 335. Note that the trigger-off level should be higher than trigger-on level by at least 2.0 ft.

Parameters in optimization models of both cases are described here. uc_i is 0.12$/kWh and *NS max* is 4. Population size is equal to 100 in the Anytown case and is 200 in the Net3 case. The generations of 5,000 are executed until termination. The parameters of operators in NSGA-II are also specified here: tournament size of two, the probability of SBX equal to 0.7, the probability of PM equal to 0.05 and the distribution index of SBX and PM being 15 and 20, respectively. It is worth noting that these parameter values were determined after a limited number of different random trials.

The optimization model was performed by 30 independent runs to avoid the influence of the randomness of initialization. The optimal solutions derived were aggregated and then extracted by the non-dominated sorting procedure (Deb *et al.* 2002).

RESULTS AND DISCUSSION

In this section, the analysis on the optimal solutions was conducted in four aspects: (1) trade-off between operational cost and resilience; (2) resilience decomposition across the optimal solutions; (3) explicit resilience assessment for the optimal solutions and (4) analysis of optimal solutions in the final Pareto set.

Trade-offs in Pareto fronts

The sets of optimal operational solutions, i.e., Pareto fronts, are shown in Figures 3 and 4 in two cases, respectively. Both Pareto frontiers basically show a clear relationship between two conflicting objectives, which indicates that the IMRI increases with the rise of the pumping cost. The reason is that a solution with the higher pumping cost can provide more surplus energy to consumers and thus improving the resilience. In the Anytown case, there exists a slight reduction of rise in resilience along the increase of pumping cost. A turning point in increase rate appears, which can guide the decision-making for pump schedule in practice. However, the growth rate of resilience in Net3 remains nearly constant over the variations of cost. It can be inferred from the distinct operational conditions between two cases, which will be illuminated concretely in the following sections.

Three solutions marked in Figure 3(b) are selected to interpret potential improvements for practical regulations. Solution A represents the currently existing regulation rules in the Net3 case, which will be illustrated in detail in Figure 7, as well as solutions B and C. In contrast to solution A, solution B in the Pareto frontier can save much cost, nearly 37.6% cost, maintaining almost the same resilience, whereas solution C can attain much higher performance progress in resilience with the

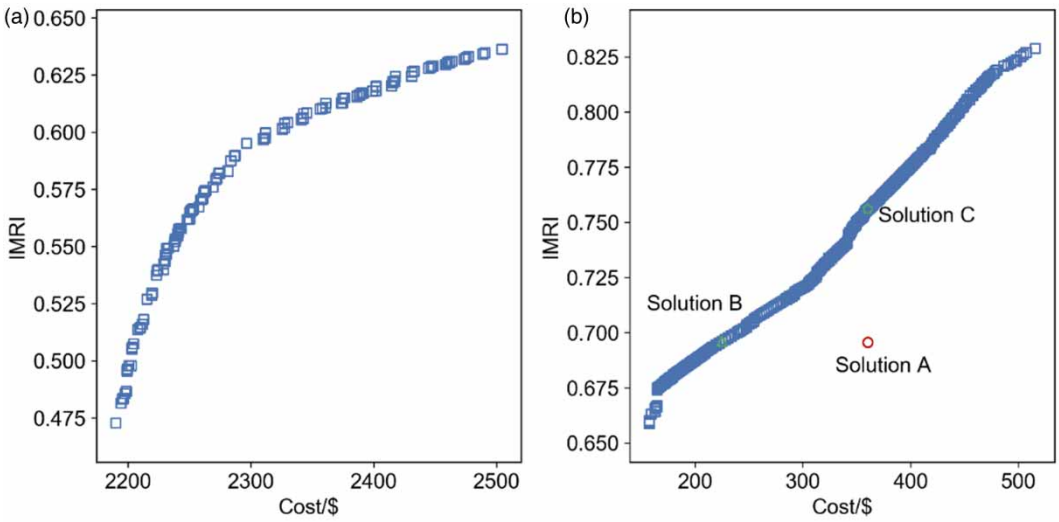

Figure 3 | Pareto fronts of the cost and the IMRI for both cases: (a) Anytown and (b) Net3.

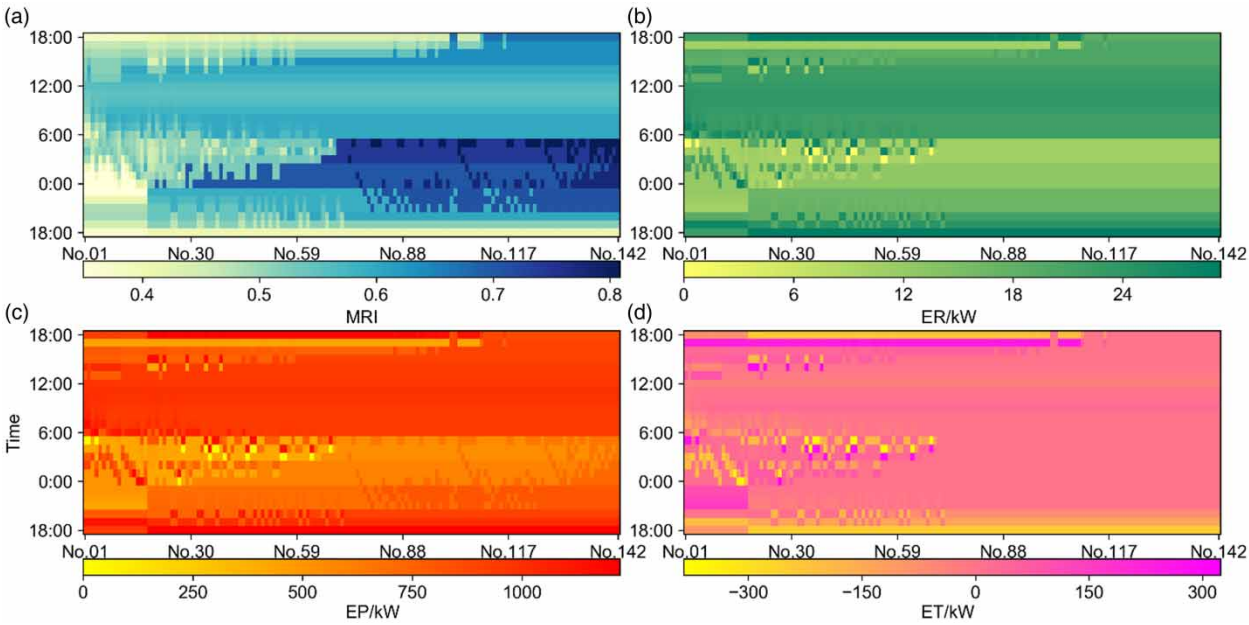

Figure 4 | Results of resilience and input energies in the Anytown case: (a) MRI evaluation; (b) input energy from reservoirs; (c) input energy from pumps and (d) input energy from tanks. Please refer to the online version of this paper to see this figure in colour: http://dx.doi.org/10.2166/aqua.2022.136.

similar cost. Therefore, these results indicate various regulation solutions of good performance for practitioners, which assemble between solutions B and C at the Pareto frontier shown in Figure 3(b).

Resilience decomposition

The comparison between resilience (MRI) and three input energy portions is investigated here, to facilitate a complementary analysis among optimal solutions. The energy portions, including reservoir, pump and tank input energies, respectively, are calculated at each hour for each optimal solution. The evaluation results of solutions in ascending order of cost are plotted in Figures 4 and 5, where the colored grids signal the hourly values. There are totally 142 optimal solutions in Pareto set for the Anytown case and 441 optimal solutions for the Net3 case. In each subgraph, the color bar below reflects the value range of each variant. In the regards of two distinct operation schedules of pump stations in Net3, Figure 6 can provide supplementary results.

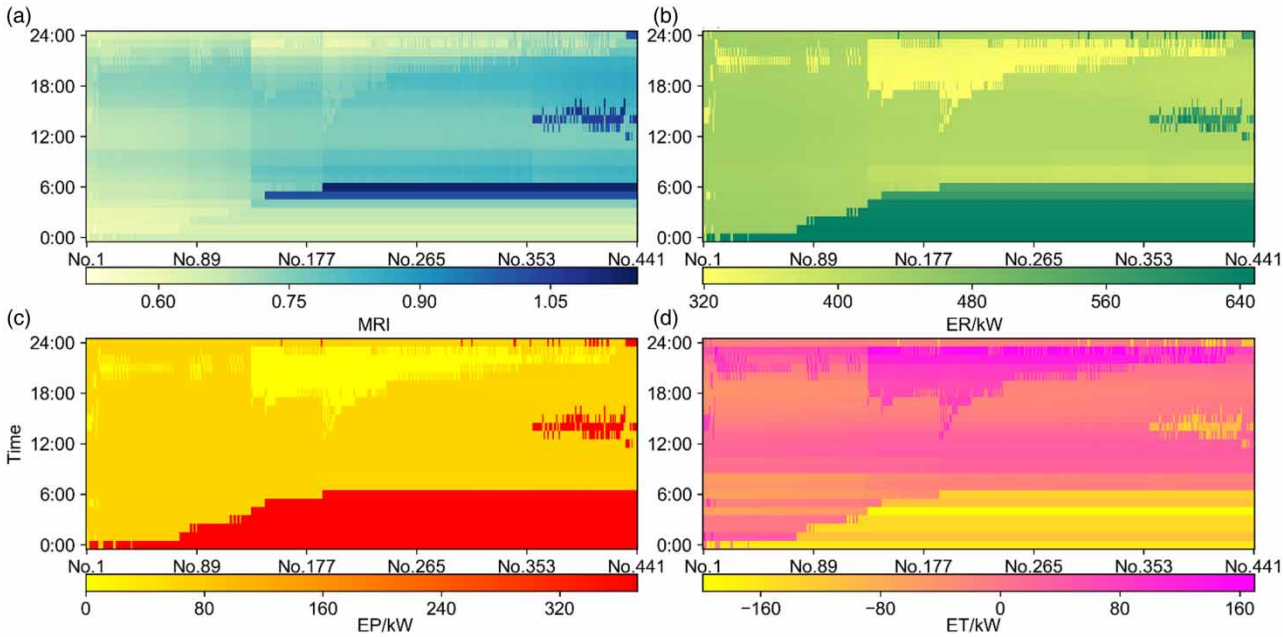

Figure 5 | Results of resilience and input energies for the Net3 case: (a) MRI evaluation; (b) input energy from reservoirs; (c) input energy from pumps and (d) input energy from tanks. Please refer to the online version of this paper to see this figure in colour: http://dx.doi.org/10.2166/aqua.2022.136.

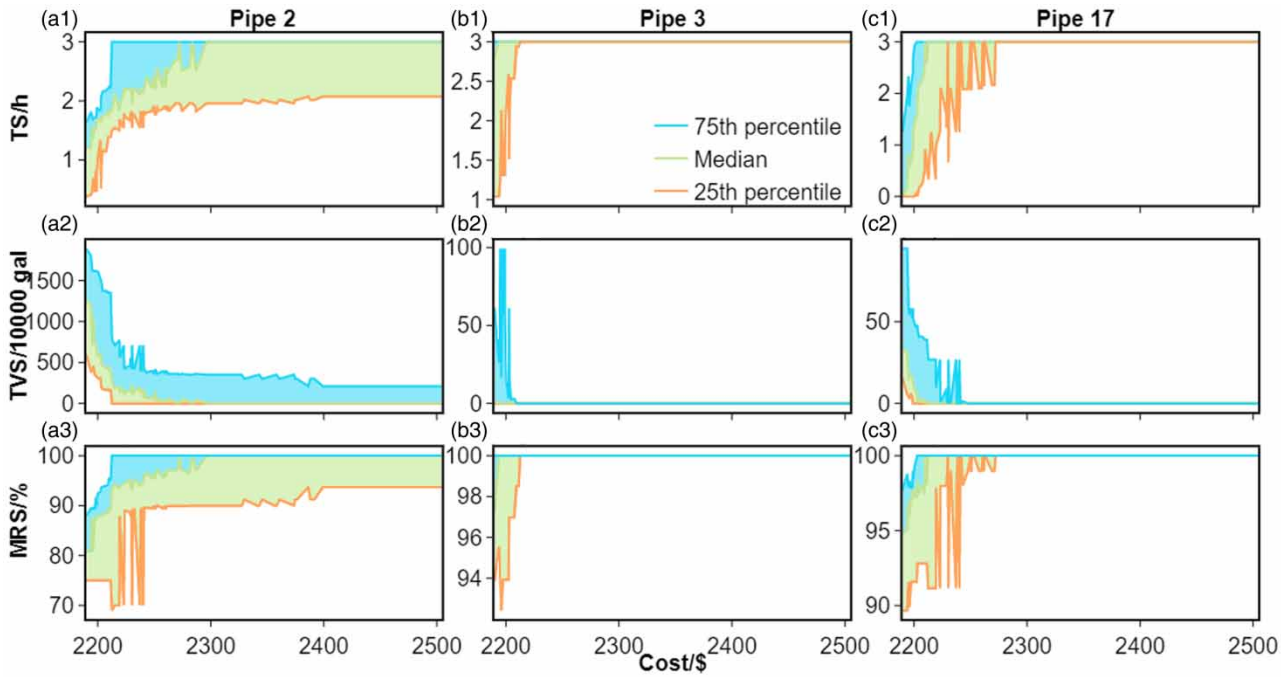

Figure 6 | Resilience evaluation under pipe failures in the Anytown case.

As expected in Figures 4 and 5, the increase of the MRI value and input energies appears at most time following with high IMRI, which is in the same ascending order of cost. It is evident that much redundant energy and reserved energy for subsequent water supply in tanks can promote the resilience performance. The subgraphs for both cases show that variation of three energy inputs between solutions has great consistency at the same time. More specifically, when more energy is supplied by pumps and their upstream reservoirs which are seen as the darker colors of grids in Figure 4(b) and (c), tanks feed less energy as seen the lighter shadings of grids in Figure 4(d).

Although the overall darker trend in grid color of MRI as *ER* and *EP* along with the rise of the IMRI, they do not exactly have a consistent relationship at the same time. The required demand at different time intervals is an important reason. During the off-peak-demand period, less energy requirements can bring out much greater improvements on MRI values than during the higher-demand periods with the same quantity of energies inputs. For instance, in Figure 4(a), the MRI in the high-cost solutions between No. 88 and No. 142, achieves much higher values during 21:00–6:00 than that those during 9:00–15:00, whereas the surplus energies, the sum of three input energies, are much lower.

In the Anytown case, there is a decrease trend of variation of operating conditions in all elements at the off-peak-demand time (21:00–06:00). Nevertheless, the operating conditions during the peak period are much less varied in Figure 4. It can be attributed to the fact that the strategy for energy-saving objective tends to feed water into the tanks during the off-peak period and supplement the water provision at peak-demand times. Except that, due to the base hydraulic conditions of Anytown, pumps lift the water from low-head reservoirs to high-elevation users and tanks. It could be reasonable that energy from pumps is much higher than other elements, shown by their value magnitude of each color bar in Figure 4.

Another notable difference appears in Net3 case in Figure 5. The value magnitude of *ER* in Figure 5(b) is much greater than two other variants shown from the color bar in Figure 5(c) and (d). As it is mentioned in section 'Case studies', though Pump Station 335 is switched off by trigger levels in Tank 1, River can still sustainably provide gravity flows by the bypass Pipe 330 switched open. In addition to its high-head, River can always supply a great deal of energy regardless of statuses of Pump Station 335 over the operating cycle. Hence, the dominance of energy inputs from reservoirs over the whole periods has a strong impact on resilience, leading to the approximately linear increase of resilience even in high-cost part in Figure 3(b).

By identifying the colored grids assigned with negative values in Figure 5(d), the operating process in which system filling surplus water into tanks during the off-peak-demand period (4:00–7:00) appears in most solutions, while the process of feeding water to consumers in tanks, can be easily found during another off-peak period (18:00–22:00).

Explicit resilience analysis

Under the explicit resilience assessment framework, the optimal solutions in Pareto fronts are sequentially evaluated by three indicators of *TS*, *TVS* and *MRS* in this section. The 3-h pipe failure scenarios incorporated in both cases are simulated 289 times, of which the starting time is generated by a fixed 5 min over the 24 h. Three water mains are chosen as representative failure locations according to pipe criticality. In the Anytown case, these failure pipes are Pipe 2, Pipe 3 and Pipe 17. For the Net3 case, they are Pipe 229, Pipe 175 and Pipe 123. The 25th percentile, the median and the 75th percentile of indicator results for 289 scenarios are calculated, respectively.

In Figure 6, the values in *TS* and *MRS* tend to increase along the increase of cost, while the values in *TVS* decrease accordingly. The reason is that the WDS regulated by the higher-cost operation solution has greater redundant energy to respond to the failures. Meanwhile, the variations in three indicators are steep between the lower cost solutions, but tends to be slight in high-cost region. It is reasonable that increasing the pumping cost with a low-cost budget would gain relatively many benefits from resilience. These similar features at all three pipes are well in line with the alterations of IMRI in the Pareto frontier shown in Figure 3(a). The value extents of three indicators at the same solution, varies differently among these three pipes. On the whole, failures at Pipe 2 have a more significant impact on water supply in the WDS than that at Pipe 17 and at Pipe 3. Pipe 2 is the main route from water resource to the high-elevation area.

The explicit resilience assessments in Net3 in Figure 7 under failures at Pipe 175 have similar variation to the results of Anytown in Figure 7. It is interesting to observe that the value fluctuations of *TS*, *MRS* and *TVS* under failures at Pipe 229 and Pipe 123 in Net3 seem to be more complex from those in Anytown. The value extents of *TS* are constant to zero in Figure 7(a1) and not in a raise as expected. That shows all failures at Pipe 229 induce the immediate deterioration in water supply. Pipe 229 is the main route to the downstream area including Node 203, so the isolation of Pipe 229 causes the disconnection of water provision to Node 203 momentarily and the vast water loss also seen from the value extent of *TVS* and *MRS* in Figure 7(a2)–(a3).

Under multiple failures at Pipe 123, Figure 7(c2) displays the sudden rise in the values of *TVS* beginning at solution No.133, which is different from the results of *TVS* at other pipes. Like Pipe 175, Pipe 123 is located at the upstream of a majority of water users and conveys large energy to the downstream in virtue of its great flow and large diameter. But Pipe 123 has smaller-diameter adjacent pipelines and less closed loops to downstream area than Pipe 175. This could be the most essential reason about the difference.

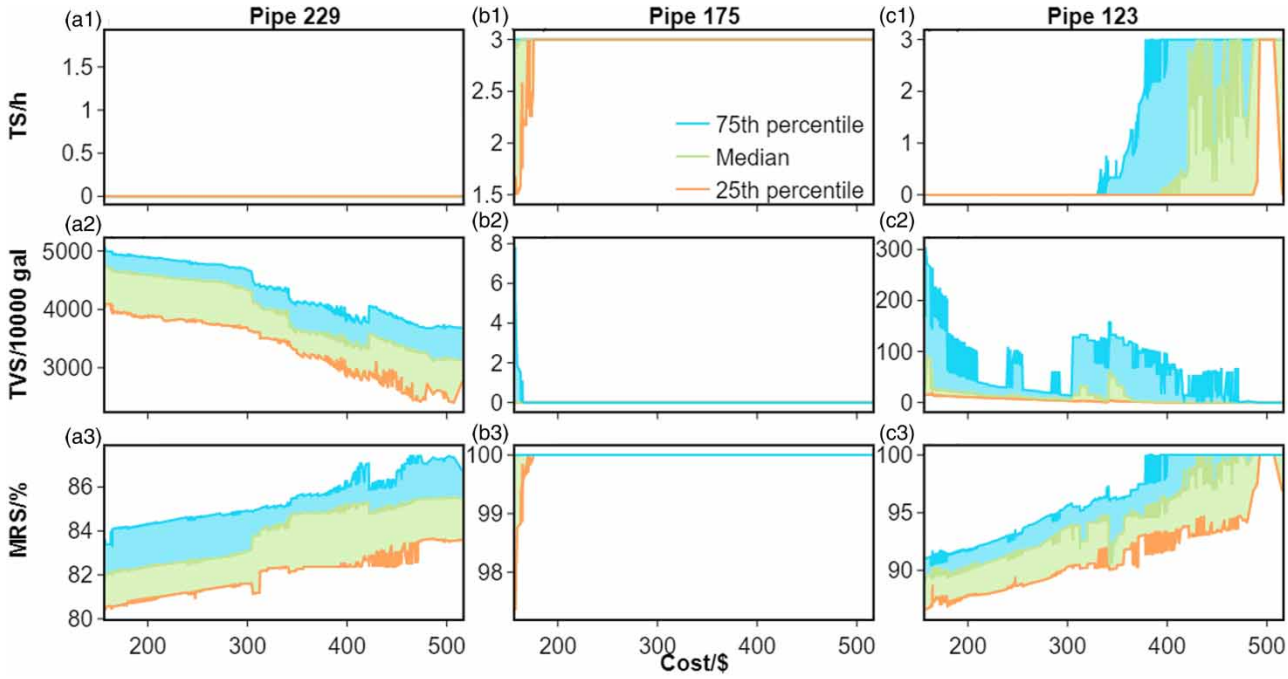

Figure 7 | Resilience evaluation under pipe failures in the Net3 case.

Solution analysis

Figure 8 reveals the optimal solutions in the Pareto set, which includes the time-table schedules of Pump Station 10, the trigger-level control rules of Pump Station 335 and the corresponding time-table schedules. On the whole, Pump Station 10 in Figure 8(a) is switched on for a longer period than Pump Station 335 in Figure 8(b) in the drive to energy-saving purpose, owing to the lower head capacity of Pump Station 10. For the same reason, the overall variations of *ER* in Figure 5(b) and *EP* in Figure 5(c) are basically in accordance with schedules on Pump Station 335. In terms of trigger levels controlling Pump Station 335, Figure 8(c) indicates that the trigger-on levels tend to ascend on average, similar to the trend of resilience. Linked to Figure 5(d), it could be inferred that the higher trigger-on level of Tank 1 is, the more reserved energy in tanks and surplus energy of system is. Meanwhile, the variation of RTC (range of trigger-level control) is exactly coordinated with the time-table schedule in which Pump Station 10 is switched off.

Figure 8 can also provide reasonable clue for the unexpected upsurge in values of *TVS* in Figure 7(c2), where it exists at solution No. 133 (the corresponding cost is 305.58$ in Figure 8(c)). Compared with the lower cost solutions, the trigger-on level in solution No. 133 is barely a bit higher in Figure 8(c) and the energy inputs from Pump Station 335 are nearly even in Figure 8(b). The much larger quantity of water shortage could be deduced from the shutdown of Pump Station 10 over more time during the off-peak-demand period, with less energy reserved to complement the water supply after the isolations for Pipe 123. Additionally, the continuous growth of *MRS* across all the solutions in Figure 7(c3), shows a consistent trend of trigger-on levels in Figure 8(c). *MRS* represents the lowest degree of actual water supply under abnormal conditions. It relates to the minimal head at each node, which a WDS could guarantee by the trigger-on level.

Some purely circumstantial inspections through comparison of three typical solutions, marked in Figure 3(b), are presented here. In Figure 9, real-time operating conditions in the WDS regulated by three typical solutions, are plotted. The water levels of Tank 1 in Figure 9(a) and pressure heads at Node 203 in Figure 9(c) over the whole operating cycle are distinct indicators, directly reflecting that solution C outperforms solution A and solution B has an equivalent evaluation result to solution A in resilience. Although scheduling Pump Station 10 switched on four more hours in Figure 9(b), solution C arranges Pump Station 335 switched on with two less hours in contrast to solution A, which can be observed with the intersecting points of RTC and the curve of water level in Figure 9(a). Consequently, they still have similar costs in this manner. Similarly, a lower trigger-off level in solution B reduces an operational time of nearly 6 h on Pump Station 335 compared with solution A, which proves that solution B shows much better in energy saving.

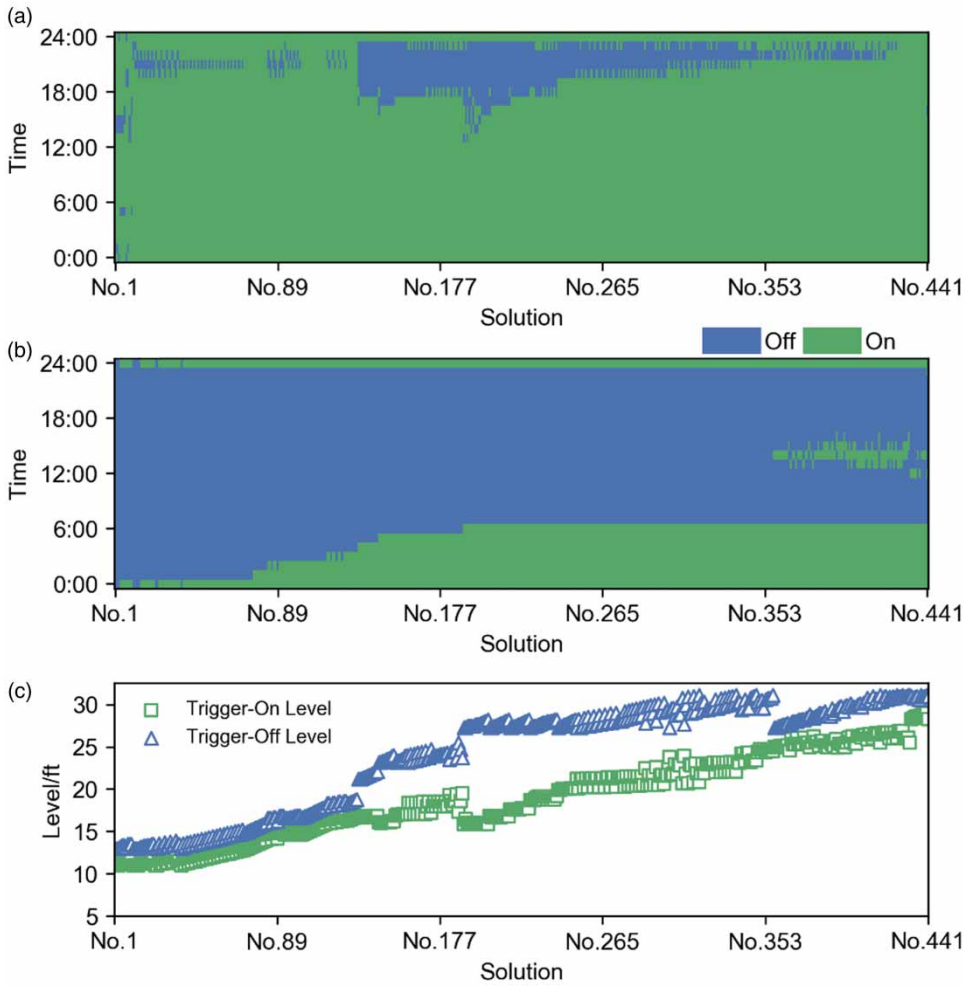

Figure 8 | Optimal solutions in the Pareto set for the Net3 case: (a) time-table schedule for Pump Station 10; (b) real-time-schedule for Pump Station 335 and (c) trigger levels for Pump Station 335.

The percentile values for three explicit resilience assessments of these solutions are summarized in Table 1, which corroborate the preceding observations. It is clear to identify that solution C is more advantageous in water supply under pipe failures while remaining nearly as economical as solution A. Solution B is significantly more cost effective and has no discernible disadvantage in terms of resilience evaluations over solution A. Examination of solutions B and C demonstrates that the optimal solutions developed using the methods outlined above are capable of balancing preferences for resilience performance and energy savings. Following these instances, water utility practitioners can use the Pareto front set to guide practical regulation by selecting targeted solutions between solutions B and C in Figure 3(b).

CONCLUSIONS

This paper presented a multi-objective optimization model on WDS operation integrated with resilience, by minimizing the operational cost and maximizing the overall resilience during EPS. A new formulation specified for resilience assessment over the operational cycle, termed as the IMRI, was proposed. Then, methods of resilience decomposition, based on the expression of IMRI, were employed to investigate the operating features of reservoirs, pumps and tanks in optimal solutions obtained by resolving the model. Finally, the resilience performances of optimal solutions obtained from optimization were directly examined under the framework of explicit resilience analysis. This framework was developed by evaluating the actual water demand under pipe failures using the following three indicators: (1) sustained duration, which stands for the time of the WDS maintaining the normal supply before water deficiency occurs; (2) total water shortage, which denotes total amount

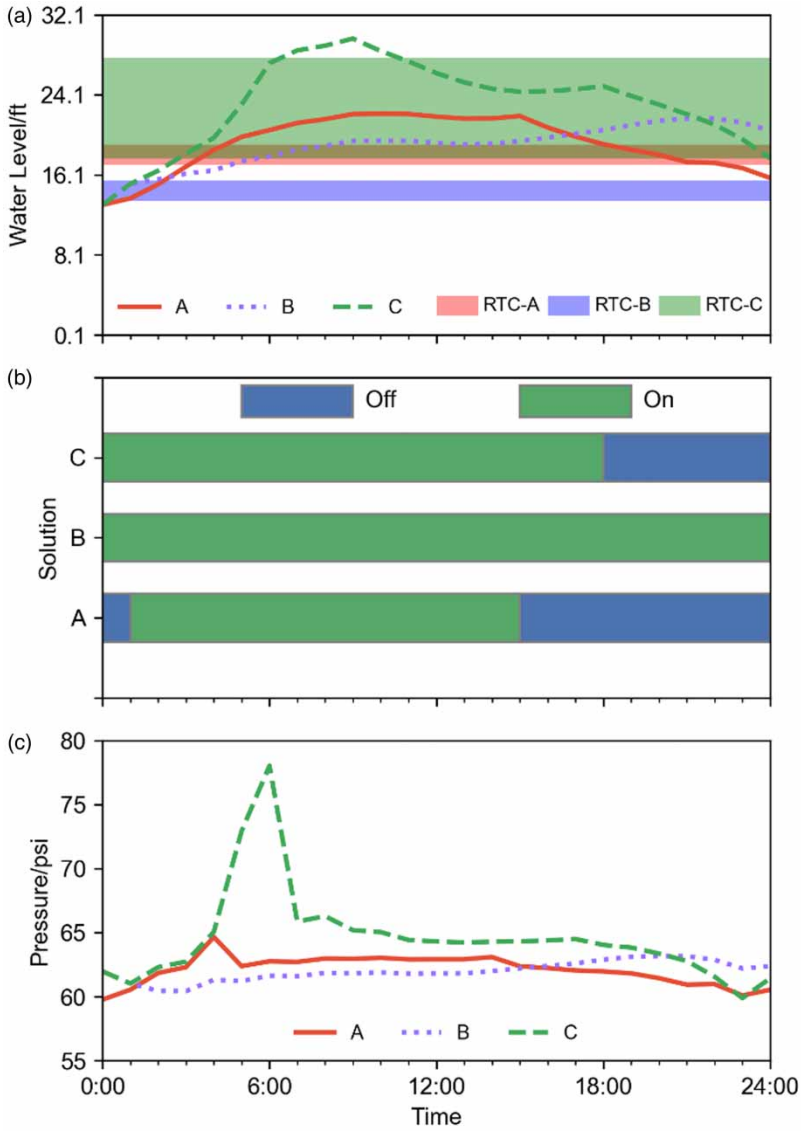

Figure 9 | Features of the three typical solutions in the Net3 case: (a) real-time water levels and RTC in Tank 1; (b) time-table schedule of Pump Station 10 and (c) pressure head at Node 203.

Table 1 | Comparison between three solutions in explicit resilience assessment under failures at Pipe 229

			TS/h			*TVS*/10,000 gal			*MRS*/%		
Sol	C_e	**IMRI**	**Q1**	**Q2**	**Q3**	**Q1**	**Q2**	**Q3**	**Q1**	**Q2**	**Q3**
A	360.36	0.6955	0	0	0	3881.12	4381.43	4704.43	80.97	83.18	84.43
B	224.87	0.6961	0	0	0	3818.48	4532.64	4843.41	81.10	82.54	84.50
C	360.17	0.7560	0	0	0	3203.65	3603.49	4101.02	82.36	84.81	85.63

unable to satisfy the required demand and (3) minimal rate of supply, which describes the lowest degree of actual water supply.

The aforementioned methodology was demonstrated in both cases of Anytown and Net3. The results show that there is a clear trade-off between the cost and the IMRI among the optimal solutions in both case studies. Resilience can be enhanced with the increase of total operational cost budget. After resilience decomposition was conducted, dynamic operating

conditions are characterized at each regulation step to give intuitive guidance for decision-makings. The evaluation results under the explicit resilience analysis indicate the rough variations in three indicators to IMRI. It can be concluded that the IMRI is capable of quantifying the overall resilience assessment for WDS operation. It is also noteworthy that in the Net3 system controlled by trigger levels in tank, trigger levels make a great contribution to resilience performance in operation. The results verify that the trigger-on level determines the largest shortage of water supply and RTC has a positive correlation with the period of sustaining normal supply.

It will be necessary to involve comparisons of multiple resilience measures applied to operation optimization in WDSs in the future work. To highlight the application of operational regulation for water utilities, the cost objective considered need to be developed to account for non-fixed electricity tariff. Pipe failures taking the probability theory into account need to be included in the resilience assessment. Meanwhile, interventions from valves during pipe failure events need to be considered in large-scale WDS cases.

ACKNOWLEDGEMENTS

This study was financially supported by the National Natural Science Foundation of China (52079016, 52122901) and the Fundamental Research Funds for the Central Universities (DUT21GJ203). The authors are sincerely grateful to Mark Morley, who developed the PDD hydraulic solver and provided us the source codes.

CONFLICT OF INTEREST STATEMENT

The authors declare that there is no conflict of financial interest or non-financial interest with any organization or entity.

DATA AVAILABILITY STATEMENT

All relevant data are included in the paper or its Supplementary Information.

REFERENCES

Atkinson, S., Farmani, R., Memon, F. A. & Butler, D. 2014 Reliability indicators for water distribution system design: comparison. *Journal of Water Resources Planning and Management* **140** (2), 160–168.

Barán, B. n., von Lücken, C. & Sotelo, A. 2005 Multi-objective pump scheduling optimisation using evolutionary strategies. *Advances in Engineering Software* **36** (1), 39–47.

Brdys, M. A. & Chen, K. 1995 Set membership estimation of state and parameters in quantity models of water supply and distribution systems. *at-Automatisierungstechnik* **43** (2), 77–84.

Brion, L. M. & Mays, L. W. 1991 Methodology for optimal operation of pumping stations in water distribution systems. *Journal of Hydraulic Engineering* **117** (11), 1551–1569.

Butler, D., Ward, S., Sweetapple, C., Astaraie-Imani, M., Diao, K., Farmani, R. & Fu, G. 2017 Reliable, resilient and sustainable water management: the Safe & SuRe approach. *Global Challenges* **1** (1), 63–77.

Coulbeck, B., Orr, C. & Brdys, M. 1987 An hierarchical approach to optimised control of water distribution systems. *IFAC Proceedings Volumes* **20** (9), 393–398.

Damelin, E., Shamir, U. & Arad, N. 1972 Engineering and economic evaluation of the reliability of water supply. *Water Resources Research* **8** (4), 861–877.

Deb, K., Pratap, A., Agarwal, S. & Meyarivan, T. 2002 A fast and elitist multiobjective genetic algorithm: NSGA-II. *IEEE Transactions on Evolutionary Computation* **6** (2), 182–197.

Diao, K., Sweetapple, C., Farmani, R., Fu, G., Ward, S. & Butler, D. 2016 Global resilience analysis of water distribution systems. *Water Research* **106**, 383–393.

Farmani, R., Walters, G. A. & Savic, D. A. 2005 Trade-off between total cost and reliability for Anytown water distribution network. *Journal of Water Resources Planning and Management* **131** (3), 161–171.

Haimes, Y. Y. 2015 *Risk Modeling, Assessment, and Management*. John Wiley & Sons, NJ, USA.

Holling, C. S. 1973 Resilience and stability of ecological systems. *Annual Review of Ecology and Systematics* **4** (1), 1–23.

Jayaram, N. & Srinivasan, K. 2008 Performance-based optimal design and rehabilitation of water distribution networks using life cycle costing. *Water Resources Research* **44** (1), W01417.

Kapelan, Z. S., Savic, D. A. & Walters, G. A. 2005 Multiobjective design of water distribution systems under uncertainty. *Water Resources Research* **41** (11), W11407.

Kurek, W. & Brdys, M. A. 2006 Optimised allocation of chlorination stations by multi-objective genetic optimisation for quality control in drinking water distribution systems. *IFAC Proceedings* **39** (14), 232–237.

Lansey, K. E. & Awumah, K. 1994 Optimal pump operations considering pump switches. *Journal of Water Resources Planning and Management* **120** (1), 17–35.

Liu, H., Savić, D., Kapelan, Z., Zhao, M., Yuan, Y. & Zhao, H. 2014 A diameter-sensitive flow entropy method for reliability consideration in water distribution system design. *Water Resources Research* **50** (7), 5597–5610.

Liu, H., Savić, D. A., Kapelan, Z., Creaco, E. & Yuan, Y. 2016 Reliability surrogate measures for water distribution system design: comparative analysis. *Journal of Water Resources Planning and Management* **143** (2), 04016072.

Lopes, R. F., Antunes, D. & da Conceicao Cunha, M. 2012 Multiple-criteria decision analysis for proactive management of risk of water distribution systems. *WDSA 2012: 14th Water Distribution Systems Analysis Conference*, 24–27 September 2012 in Adelaide, South Australia: Engineers Australia, p. 1055.

López-Ibáñez, M., Prasad, T. D. & Paechter, B. 2008 Ant colony optimization for optimal control of pumps in water distribution networks. *Journal of Water Resources Planning and Management* **134** (4), 337–346.

Mala-Jetmarova, H., Barton, A. & Bagirov, A. 2014 Exploration of the trade-offs between water quality and pumping costs in optimal operation of regional multiquality water distribution systems. *Journal of Water Resources Planning and Management* **141** (6), 04014077.

Morley, M. S. & Tricarico, C. 2008 *Pressure-Driven Demand Extension for EPANET (EPANETpdd)*. University of Exeter, Exeter, Devon.

Odan, F. K., Ribeiro Reis, L. F. & Kapelan, Z. 2015 Real-time multiobjective optimization of operation of water supply systems. *Journal of Water Resources Planning and Management* **141** (9), 04015011.

Prasad, T. D. & Park, N.-S. 2004 Multiobjective genetic algorithms for design of water distribution networks. *Journal of Water Resources Planning and Management* **130** (1), 73–82.

Raad, D., Sinske, A. & Van Vuuren, J. 2010 Comparison of four reliability surrogate measures for water distribution systems design. *Water Resources Research* **46** (5), W05524.

Rossman, L. 1993 *Epanet Users Manual*. Environmental Protection Agency, Washington, DC, USA.

Rossman, L. A. 2000 *EPANET 2: Users Manual*. Environmental Protection Agency, Cincinnati, OH, USA.

Todini, E. 2000 Looped water distribution networks design using a resilience index based heuristic approach. *Urban Water* **2** (2), 115–122.

USEPA 2008 *Ensuring A Sustainable Future: An Energy Management Guidebook for Wastewater and Water Utilities*. Available from: https://www3.epa.gov/npdes/pubs/pretreatment_ensuring_sustainable_future.pdf (accessed 3 October 2021).

Walski, T. M., Brill Jr, E. D., Gessler, J., Goulter, I. C., Jeppson, R. M., Lansey, K., Lee, H.-L., Liebman, J. C., Mays, L. & Morgan, D. R. 1987 Battle of the network models: epilogue. *Journal of Water Resources Planning and Management* **113** (2), 191–203.

Wegley, C., Eusuff, M. & Lansey, K. 2000 Determining pump operations using particle swarm optimization. *Building Partnerships, Joint Conference on Water Resource Engineering and Water Resources Planning and Management*, 2000. ASCE, Minneapolis, pp. 1–6.

Zessler, U. & Shamir, U. 1989 Optimal operation of water distribution systems. *Journal of Water Resources Planning and Management* **115** (6), 735–752.

Zhuang, B., Lansey, K. & Kang, D. 2012 Resilience/availability analysis of municipal water distribution system incorporating adaptive pump operation. *Journal of Hydraulic Engineering* **139** (5), 527–537.

First received 10 October 2021; accepted in revised form 14 March 2022. Available online 12 April 2022